Tectonics of Small bodies

P. Thomas, L. Prockter

1. Introduction: Types of small bodies, their properties and environments

Small bodies of the solar system are here taken to be those too small for gravitationally-driven viscous relaxation to have determined their shapes. This definition restricts consideration to objects less than about 150 km radius (Johnson and McGetchin 1973; Thomas 1989). Within this definition are some dozens of satellites of planets, and thousands of asteroids, cometary nuclei, and Centaur and Kuiper-Edgeworth belt objects Binzel et al. 2003). As of late 2003 spacecraft have visited small satellites, asteroids, and two cometary nuclei. Resolved information on these objects is dominated by the NEAR mission that orbited and then landed on 433 Eros, and by images of the Martian satellites, Phobos and Deimos. Radar images of near-earth objects are beginning to show some details of asteroid shapes and surface features (Hudson et al. 2003). Meteorites provide small samples of asteroids, though only in the case of asteroid Vesta are there positive connections of meteorite samples to a specific object (Binzel et al. 1997; Keil, 2002).

Interest in these small bodies stems from a desire to fit them in the sequence of formation and modification of all solar system bodies. Large planets undoubtedly formed from accumulations of smaller components, and subsequently continued impacts of small objects have perhaps modified the chemistry and surfaces of planets. On earth impacts are associated with features as diverse as ore-body initiation to global biologic extinctions. Study of small bodies is advanced enough that interpreting their history and internal makeup are required to evaluate their past and future effects on planets. For instance, are most asteroids loose accumulations of fragments, or are they monolithic?

Even with spacecraft visits, this question has been difficult to answer positively, and many indirect methods, such as orbital dynamics of remnants of catastrophic collisions, are used to infer asteroid structures.

2. Small bodies: characteristics

Asteroids

While most asteroids orbit the sun between Mars and Jupiter, gravitational perturbations of planets place some into more eccentric orbits that cross those of the inner planets, with collisions or even ejection from the solar system limiting their lifetimes. Most asteroids fall into our categorization of small objects; several thousand are between 1 and 150 km in diameter. They encompass a variety of compositions as indicated by meteorite samples and spectroscopy. Compositions include iron-nickel metals, olivine, pyroxene, plagioclase and other silicates; clays and organics, and some likely to have organics and possibly ices and other oxides. The asteroid belt is compositionally zoned, reflecting probable different condensation compositions and temperatures as a function of distance from the sun (Gradie and Tedesco 1982; Grimm and McSween 1993)). After formation, asteroids suffered orbital perturbations, collisions, and different amounts of internal heating, and in some instances, differentiation (Bell et al 1989).

Comets.

Comets are distinguished by having significant volatile components. They have been perturbed into orbits that bring them to the inner solar system from reservoirs tens of AU distant (Kuiper belt) or from much father out (Oort cloud). Their lifetimes in the inner solar system are geologically brief, chiefly due to volatile loss, but also due to impacts in to planets and the sun. Volatile compositions include water ice, CO_2 , CO, and

other “icy” compounds. Silicates and organics are part of the non-volatile component. Spacecraft imaging, and behavior observed from the ground, show that the great majority of comet surfaces are dark (albedo of a few percent), non-volatile materials. Fractional areas of comet surfaces actively sublimating due to solar radiation are relatively small (A’Hearn et al. 1992). Comet nuclei are generally a few km across; 20 km length is a very large comet.

Small satellites.

Small satellites may be composed of materials formed with the parent planet, or objects captured into orbit around the planet. Compositions are poorly known, with some approximate spectral comparisons being the best available information, such as for the martian satellites. In general, small satellites close to the primary, in circular orbits are thought to have formed with the planet; those in distant, elliptical, and inclined orbits are likely to have been captured into orbit and may be asteroidal or cometary bodies.

3. Stress environments of small bodies

On the Earth and other terrestrial planets, most tectonics are driven by stresses of internal origin, in most cases ultimately tied to thermally driven convection. The small size of the objects we are considering limits any thermal convective activity to very early in their history, when exotic heat sources, such as short-lived radionuclides (Grimm and McSween 1993), or inductive heating (Sonnett et al. 1968) may have occurred in some objects. The presence of iron-nickel meteorites, and other mineral compositions requiring some melting and differentiation, shows that at least some bodies did experience some periods of thermal activity, with likely accompanying stresses. Our opportunity to detect structures resulting from such activity is limited by the subsequent

impact processing of these bodies that has in many instances apparently stripped silicate mantles from metallic cores, and disaggregated mantle materials and large scale structures.

Thermal evolution of cometary bodies is even less well known, and probably of a very different character from that of asteroids, as their initial large distances from the sun and high volatile content reduce the chances for solar or internal heating. Additionally, for many of the volatiles the low internal pressures mean that transition of phases may involve solid-gas rather than solid liquid changes. (some solid state phase changes are possible), thus making convective structures unlikely. As will be noted below, though, comets may be so weak that very small stresses associated with volatilization may be effective modifiers of their structures.

Impact environment

Collisions among small bodies, asteroids, comets, and small satellites, provide the highest stresses suffered by these objects. Velocities of objects in different solar orbits can vary tremendously, but relative velocities of 5-10 km/s are common in the asteroid belt and inner solar system. The cratering event can be divided into three stages: contact and compression, excavation, and modification (Gault et al. 1968; Melosh, 1989). Upon contact with the target, both are compressed generating shock waves that propagate into both objects. Pressures developed during high velocity impacts commonly reach hundreds of GPa, far above yield strengths for target and projectile. This stage lasts only as long as it takes the shock wave to traverse the projectile, perhaps milliseconds for an objects tens of meters across. During the excavation stage, the shock wave expands into the target, it and the following rarefaction put target material in motion, which lasts much

longer than the compression stage. After excavation, the “transient” crater, is modified by gravity, with material slumping into the crater to define a final profile. Structurally, the importance of this process is the application of high stresses, and high strain rates, for a volume of the target somewhat larger than the final crater. Some material is melted and vaporized, fractures can extend several crater radii out, and some materials are very highly compressed and otherwise strained. The resulting crater’s depth is approximately half due to excavation of material, and half due to compression or other flow within the target body (Melosh 1989).

The ultimate impact outcome is dispersal of the target object in many pieces that exceed the escape velocity of the object’s mass. All but the largest asteroids, and most probably all of the small bodies that we are considering, are the result of impact fragmentation and are themselves subsequently cratered. Crater populations approximate size-number distributions expected of products of collisional fragmentation (Chapman and McKinnon 1986); thus there is a mutual grinding down of the small objects over geologic time. The fragmentary origins of many asteroids are also inferred from observations of families of asteroids in similar orbits, apparently formed by breakup of a parent object. The irregular shapes of many asteroids also suggests fragmentation origins.

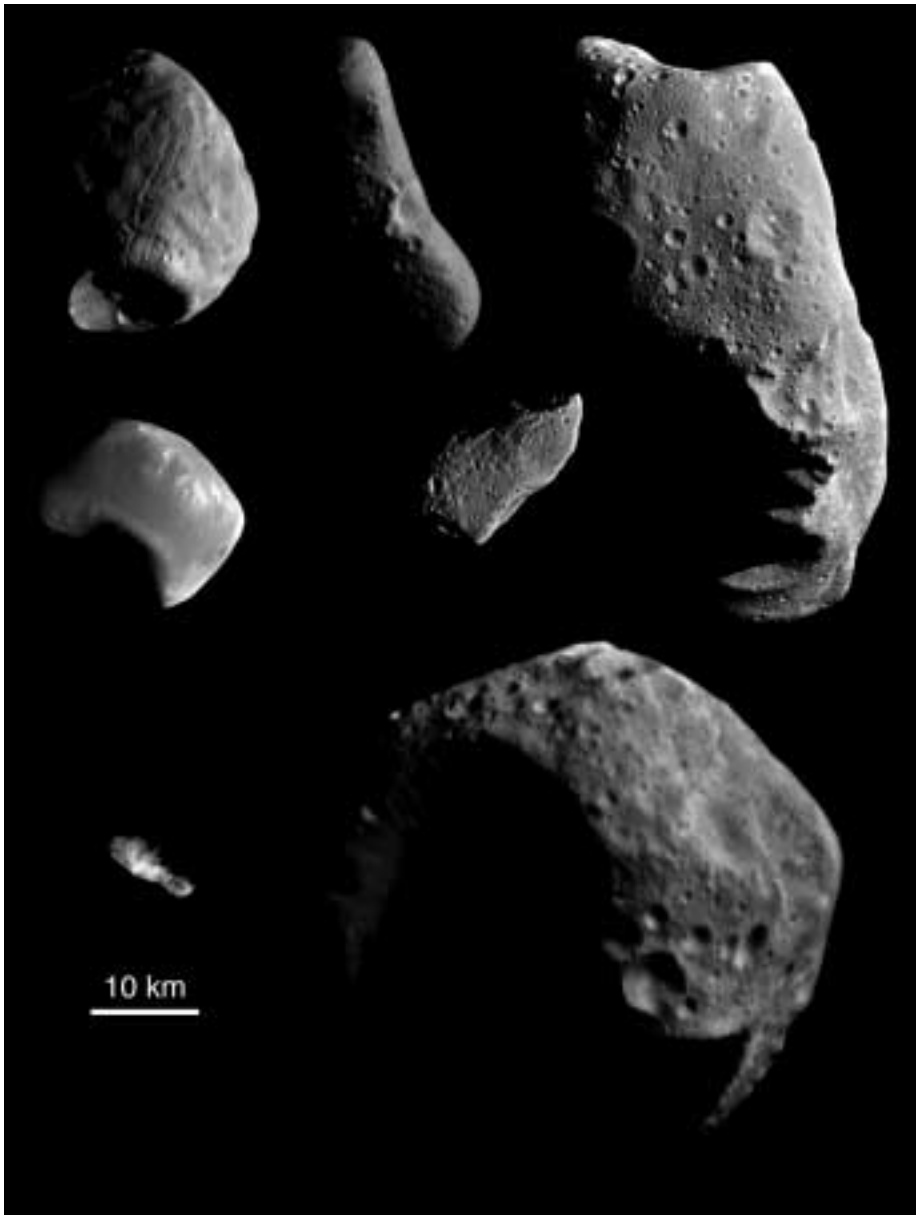

Figure 1. A sampler of small solar system objects. Top row, left to right: Phobos, Eros, Ida. Second row: Deimos and Gaspra. Bottom row: comet Borrelly and asteroid Mathilde.

Tidal stresses

Stresses may be induced in small objects by the gradient of gravitational acceleration due to another, usually larger, object. For asteroids, these stresses are

usually imposed during the occasional close encounters with much larger planets, but can be induced by close encounters with other asteroids.

For satellites, tidal forces are always present, and may change over time due to evolution of the orbit toward or away from the planet. The period of the satellite's orbit is determined by the distance of the center of mass to the primary, yet parts of the satellite that are closer or farther from the planet are forced to have the same orbital period as the center of mass. This imposes a slight tensional stress along the vector to the planet. The majority of satellites are locked into a spin period equal to their orbital period, thus these stresses along the object, although weak, may act for long periods of time. They also may provide a stress field that may combine with other stresses. The magnitude of these stresses, is quite small. For instance, modeling by Dobrovolskis of the 27 km long satellite Phobos yields tidally imposed deviatoric stresses of order 100 mbars. Central pressure in Phobos is on the order of 700 mb.

For asteroids and comets, close encounters with planets can provide short periods of tidal stress; these are hypothesized to affect the distribution of loose material on some asteroids, and even their shapes (Bottke et al.;1999). Some comets are known to break apart under tidal stresses, most notably Shoemaker-Levy 9 (Asphaug and Benz 1996). In the cometary examples, tidal stresses can be less than 100 dyne/cm^2 and still effect disruption of km sized objects. This behavior has been used to infer extremely low tensile strengths for comets, and even a distribution of sizes of agglomerated particles or, fracture spacing within the object.

Thermal stresses

Thermal stresses within asteroids may arise from insolation variations of daily rotation and seasonal variation of solar insolation, and seasonal variation due to elliptical orbits. The depth over which these stresses operate is determined by the period of insolation variation (length of seasons) and on the thermal inertia of the surface materials. Long term orbital changes might generate global temperature gradients that could induce a few MPa stress on a 10 km object (Dombard and Freed 2003), but this requires a globally coherent object. Any thermal stresses are likely to be induced in the loose material (regolith) covering the object. Effects are most likely expressed as downslope creep of loose material, rather than as large scale fracturing or tectonics. Thermal effects on the lunar regolith have been studied by microseismicity (Duennebier 1976), and have been suggested to apply to small objects such as Deimos and Eros.

On comets, the effect of variable solar insolation is largely taken up by variations in evolution of volatiles, and sometime strong heating of the very dark, non-volatile crusts that develop (Soderblom et al. 2002.). Significant fracturing and even break up may develop due to stresses associated with elevated vapor pressures. However, observed breakup of comets has been difficult to associate with onsets of heating.

4. Observing structures in small bodies: methods and limitations

The nature of asteroid and cometary exploration so far limits us to remote detection of structures and tectonic features. Remote sensing of small bodies consists of visible and infrared imaging, radar imaging, and one instance of laser altimetry. Table 1 briefly summarizes the types and quality of data available for some of the well-resolved objects of concern here.

The most fundamental limitation on remote sensing of satellite and asteroid structures is the presence of regolith. Here we use "regolith" to be any of the loose material, of whatever origin or particle size, on the surface. Virtually all regolith on these objects is probably the result of impact fragmentation. Despite the low gravity on objects only a few km across (typically of order 10^{-3} that on the Earth), cratering does leave significant fractions of the excavated material as distributed debris, apparently including fine grained components. On parts of Eros regolith is estimated to be over tens of m deep (Robinson et al. 2002), and possibly over 100 m in places on the Martian satellites (Horstmann and Melosh 1989; Thomas 1998). This covering has much the same camouflage effect that soil, alluvium, or other surficial debris does on seeing terrestrial features. However, as with the earth, the covering can respond to topography and motion of the more solid substrate, and thus structures of some sort have been mapped on most of the small bodies imaged close up. Interpretation of this response is one of the major hurdles in interpreting the structural patterns on these objects. (Section 7 below).

5. Accretional and precursor body structures

Original structures from accretion of asteroids might be present if they have not differentiated or been mechanically altered after formation. The vast majority of asteroids (<200 km diameter) are regarded as in some way fragmentary remains of larger precursor objects. A substantial fraction of these may have been differentiated in whole or in part (Grimm and McSween 1993) and would not be expected to show obvious remnants of accretion. Some asteroid classes, such as C and D classes may be thermally less processed, so there might be the possibility of remaining accretionary structures. However, from the standpoint of remote sensing, structures induced later by impact

fragmentation might be very similar to original accretionary ones. Thus indications of layering or the like have to be evaluated from the standpoint of when in the history of the object they might have been formed.

Layers in small bodies

Any small body that is a fragment of a larger precursor body might expose layering formed in that body by differentiation, accretion, or reassembly of pieces after earlier fragmentations. Accretion is usually thought to involve a range of particle sizes, including those a significant fraction of the "final" object size, so well organized, global layering is probably not accretionary, or from reassembly of pieces after fragmentation. Layering from differentiation might not be perfectly smooth, and would probably tend to have a radius of curvature appropriate to the depth within the parent body. Thus expression of parent body layers in fragments we observe today could be effectively planar to noticeably curved.

There are only three instances yet observed where layers or planar structures extend for a large fraction of an asteroid's length: Mathilde, Eros, and Ida. All of these present some interpretive complications.

Mathilde, Fig. 2, with a mean radius of ~26 km was imaged at approximately 250 m/pixel. The chief findings from the images were several impact craters with diameters equal or larger than the object's mean radius. These craters gave no evidence of ejecta deposits or of substantial deformation of older craters. The asteroid's mass determined from tracking the space craft indicated a mean density of approximately 1.3 g/cm^3. This density, in combination with the likely composition of the object, suggests a porosity of well over 30%, and possibly of order 50% (Veverka et al. 1999)

The images of Mathilde showed another remarkable surface feature: a bright marking, about 1 km wide, extending about 20 km along the surface, with at least one offset in its trend. This feature, although subtle, occurs in many images. It appears to be an albedo feature, interrupted on scales of 200-400 m by small craters (?) or other topography. As subtle as it is, it is the only real candidate among the asteroid images for something that might be called an "exposed" layer in the body of the object (As opposed to exposed regolith layers; these exist on Phobos). Given the scale of the images and possible regolith depths, even this marking may not be really exposed. The bright marking might be the locus of excavation by small craters through a regolith into an underlying feature. Craters 200 m in diameter, individually invisible at this resolution, could excavate from beneath 20-30 m of regolith, and leave a surficial trace of different materials at depth. If this marking indeed is from a layer, it suggests a structure in something originally much larger than the present size of Mathilde.

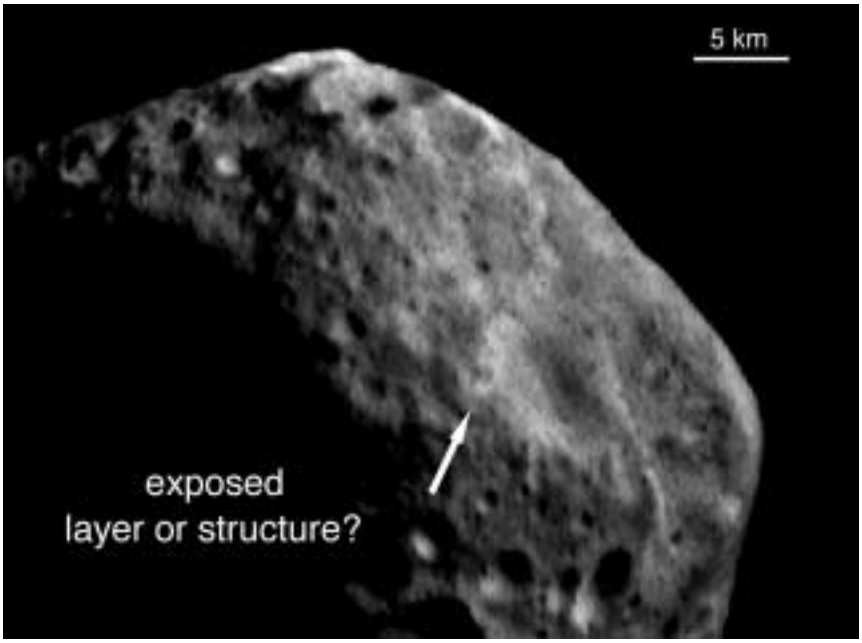

Figure 2. Mathilde, surface markings. The brighter linear feature is visible in many images, and shows no topographic expression at 120 m/pixel. It is unlike features seen on other small bodies, and might represent exposure of a layer, or crater sampling of a layer through a regolith of tens of m or less in depth. NEAR Multispectral Imager image 42826484.

Eros was thoroughly mapped by the NEAR-Shoemaker Spacecraft; nearly all the surface was imaged at better than 4 m/pixel, and parts were imaged at less than 1 m/pixel. This detailed imaging allows for definitive mapping of the presence or absence of different types of surface features. Evidence of loose material on the surface is ubiquitous as shown by both morphologic and albedo features. Early images showed suggestions of aligned features, and efforts were made to establish global patterns. Only one global pattern emerged from the mapping of surface features and asteroid shape (Fig.

3). Two structural features, a ridge (Rahe Dorsum) and a ridge/trough system (Calisto Fossae) can individually be well fit by planes, and these are coplanar. This alignment of the largest linear features on the object strongly suggests a structural link through the 22 km from Calisto Fossae to the farthest part of Rahe Dorsum (Thomas et al. 2002).

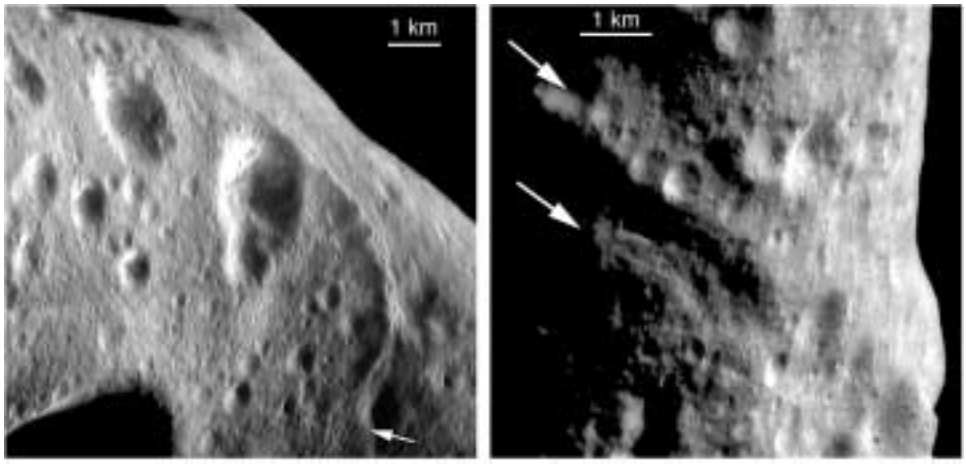

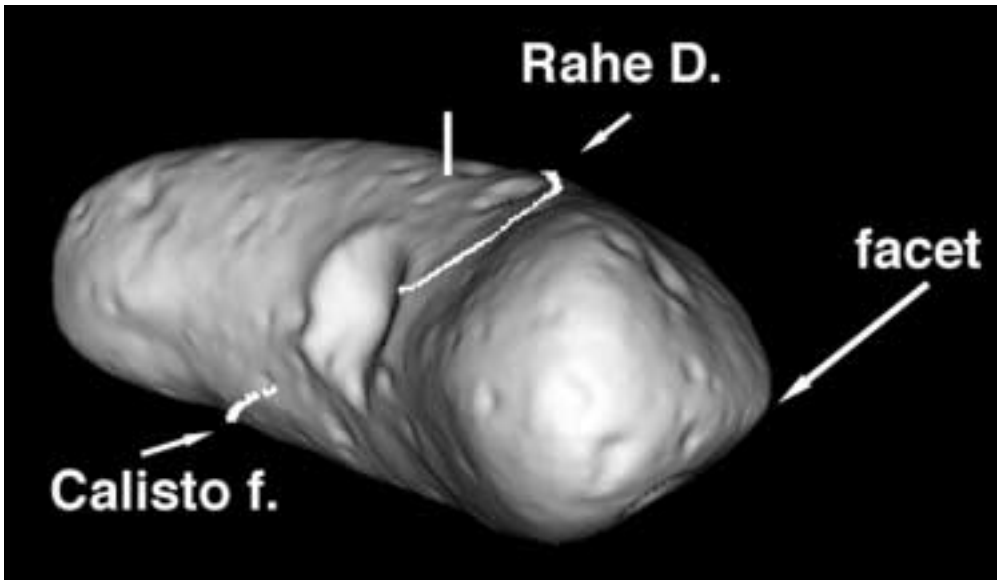

Figure 3. Global structures of Eros. a. Portion of Rahe Dorsum, showing the narrow, sinuous nature of this ridge. near crater Himeros. Images 129901617-129901897. b. Calisto fossae, a double trough-ridge feature with many superposed craters that is coplanar with Rahe Dorsum. Image 130230097. c. Relation of Rahe Dorsum, Calisto fossae, and a nearly planar facet on Eros. Image-derived shape model with mapped locations of features.

Furthermore, one of the nearly planar facets of the shape of Eros (Fig. 3), is nearly parallel (within ~7 deg) to the orientation of this plane. The detailed morphology of Rahe Dorsum and other structural expressions on Eros will be discussed below. Although these features indicate a planar structure, and possibly two parallel structural trends, there are three different morphologic expressions that probably formed at different times. The ridges and troughs in Calisto fossae are very heavily cratered, and suggest exploitation of weaknesses by the cratering process. The feature and the surface expression are very old. Rahe Dorsum has crisper topography, is much narrower, and does include a change in morphology along its length (see Sec.7 below), and it is by no means certain that all sections are of equivalent age. This feature suggests displacement along a fault rather than the morphologic exploitation by cratering. The parallel (but not coplanar) facet also may suggest exploitation of weaknesses by spallation. It may be very old as well. Thus there is a likely near-planar fabric to Eros, exploited in at least two different ways, probably at different times. This fabric is detected only indirectly, so our ability to characterize it is limited at best. The radius of curvature is very large, so if it represents inherited structure, it might indicate a substantially larger precursor object.

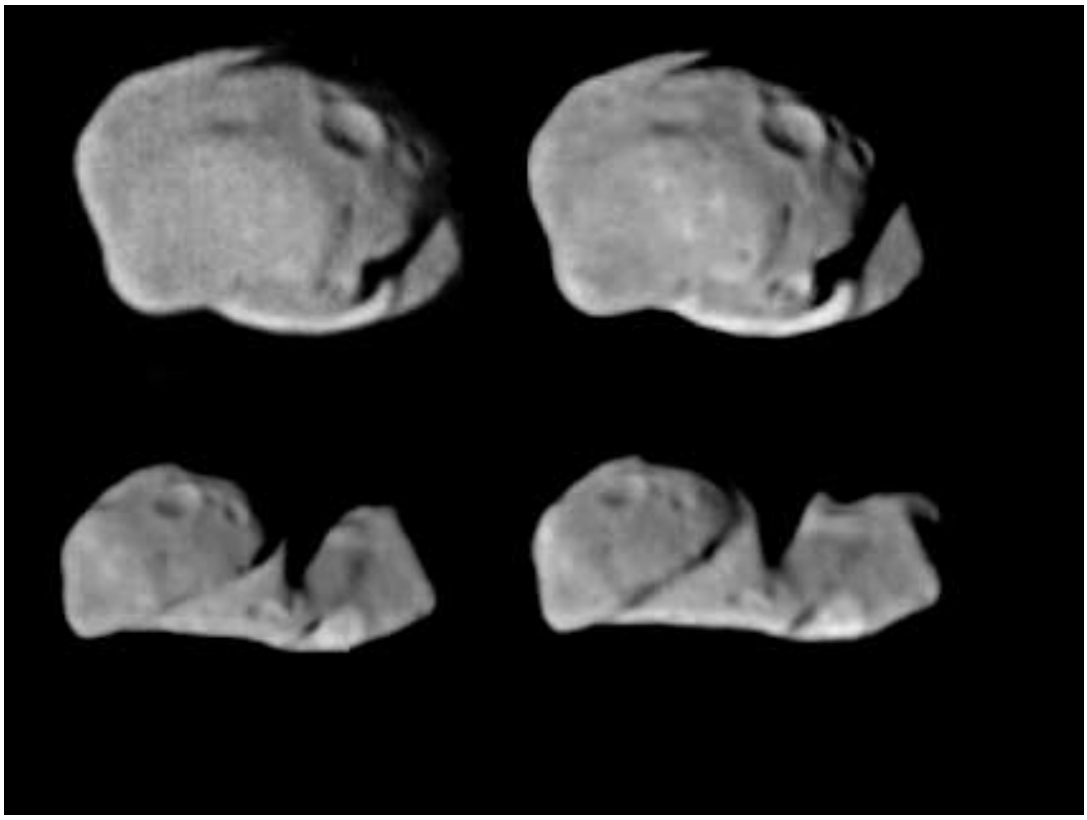

Figure 4. Stereo views of planar topographic boundary on Ida. Top view looks along the long axis of the asteroid, Vienna Regio is the concavity in end facing out. Galileo images S0202557100 and S0202557300. Bottom pair shows view from the right relative to the top pair, images S0202553700 and S0202554800.

Asteroid Ida, imaged by the Galileo spacecraft in 1993, has a mean radius of 15.7 km, a maximum length of 56 km, and a somewhat bent profile when viewed along its spin pole. In terms of global structure, it has a ridge, Townsend Dorsum that traverses 40 km and about 150 of longitude (Fig 4). The crest of this ridge is well fit by a plane

(within about a km over its length). The ridge is imaged at low resolution; one end of it just reaches an area of very much higher resolution imaging, but this area displays no discernable continuation of the feature. The ridge, especially the morphology shown in Fig 4, might suggest displacement along a fault. However the projection of the ridge into the area of high resolution data shows no sign of fault topography. Thus, it might be an older feature, such as a compositional discontinuity, that has been etched by cratering and spallation.

Binary objects

Perhaps the ultimate asteroid structural features are binary asteroids: two objects in orbit about each other. Satellites of asteroids were long suspected to exist, but after many false indications, started to be discovered in the 1990's, beginning with Dactyl orbiting Ida. Satellites of asteroids were expected to result from catastrophic and near-catastrophic impacts. Objects such as Dactyl are very small compared to the primary asteroid, but other objects more closely match the connotation of binary objects, that is, pairs of bodies of somewhat comparable sizes. Binary main belt asteroids are being found, and many of the Kuiper belt objects appear to be binary. The near-Earth asteroid population of objects may be ~1/6th binary (Margot et al. 2002). One of the early hints at a noticeable population of small binary objects was the number of binary impact craters on the Moon, Mars and other objects. These were thought to form by tidal separation of objects orbiting close to one another just before impact (Aggerwal and Oberbeck 1974).

Differentiation

The small sizes of asteroids limit the possibilities for differentiation. Nevertheless, some types of asteroids appear to represent differentiated objects, and

meteoritic evidence shows many small bodies did indeed suffer enough melting to differentiate. Those likely to have suffered melting are concentrated in the inner asteroid belt, where it is thought accretion occurred more rapidly, allowing short lived radionuclides, especially ^{26}Al, to heat them (McSween et al. 2002). Alternative suggestions of heating by electromagnetic induction remain difficult to model (Sonnett et al. 1968). However, the clear evidence of melting in the form of metallic and various silicate-rich achondritic meteorites shows that some differentiation did occur.

Melting and differentiation can generate many types of structures. These include both global shell structures, intrusive bodies of various shapes and the attendant mechanical and thermal modifications on their boundaries, faulting, and fracturing, and volcanic forms at the surface.. Metallic cores often retain structures developed in the cooling metal. Yet it is not clear that any of these structures have been detected by spacecraft. While Gaspra may be differentiated, even metal-rich, the only possible structural relation to differentiation seen might be its overall shape which is somewhat rhomboidal (Thomas et al 1996). Eros, best approximated by an LL chondrite meteorite composition, appears undifferentiated (McCoy et al. 2001)

6. Interior structure from impacts

"Rubble piles"

The expectation of catastrophic collisions having occurred for even 100 km diameter objects suggests most asteroids record features of severe fracturing or global fragmentation. A crucial aspect is the expectation that fragmentation yields a range of sizes and a range of velocities relative to the center of mass, which means that many fragments may reaccumulate under the influence of gravity. It is reasonable to expect for

larger objects, that repeated large impacts can occur on an object without dispersing it completely. A simple comparison illustrates this situation: The energy needed to fracture, to a certain fracture density (or particle size), varies essentially as the volume, or as R_m^3 (R_m = mean radius). The gravitational binding energy, however, varies as R_m^5. Thus there are size ranges where the object may be thoroughly, repeatedly, and heavily fragmented, but much of the mass can be expected to be reaccumulated.

Objects that are gravitationally bound collections of fragments have been termed "rubble piles." Recent work by Richardson et al. (2002) has attempted to classify the possible states of fragmentation of asteroidal bodies. Their classification uses porosity and relative tensile strength, which is the ratio of tensile strength of the object to the tensile strength of the components. Objects with high porosity and low strength are likely to be gravitational *aggregates*; high strength and low porosity are *monolithic* forms. Objects that have tensile strength reduced by faults or cracks yet retaining original structures are termed *fractured bodies*. *Shattered bodies* applies to those objects with fractionally large reduction in tensile stength. *Rubble piles* are those that have been shattered and reassembled. A slightly different classification has been presented by Britt et al. 2002 that divides asteroids into three general groups: those that are essentially monolithic, heavily fractured ones with macroporosities of ~20%, and loosely consolidated ones with porosities over 30%.. Structurally, the primary factors are whether any individual fragments are rotated from their "original" positions, and whether porosity is due to opening of fractures or to irregularities of packed material that has moved relative to each other.

Although there is a growing sense that a large fraction of 0.1 – 100 km sized asteroids are loosely bound aggregates, the evidence is in most measure circumstantial. Asteroid spin periods derived from lightcurves have been used to infer a lack of tensile strength for objects over 200 m in size (Pravec and Harris 2000). Asteroids, and some small satellites, appear to have large porosities on the basis of mean density and their probable compositions. Mathilde, with a density of ~1.3 gcm^{-3} is estimated to have a porosity of up to 50% (Veverka et al. 1999). Other asteroids may also have high porosities (Merline et al. 2002; Britt et al. 2002). Two icy satellites of Saturn, Epimetheus and Janus, have compositions thought to be largely water ice, and densities less than 0.7 gcm^{-3}, suggesting porosities of order 30%. Craters with diameters equal, or even greater, than the object's mean radius are common on small objects (Thomas 1999). Hydrocode modeling of these impacts predicts that they can form only in fractured or weak targets (Asphaug et al. 1998). Shapes of asteroids that display low gravitational slopes below an angle of repose have also been suggested to imply loose materials (Ostro et al. 2000). Objects with a somewhat s-shaped profile viewed along the spin axis might be consistent with reassembly after tidal breakup (Bottke et al 1999), and thus may indicate a loose constitution. More circumstantial evidence comes from doublet craters (Aggarwal and Oberbeck 1974) and asteroid families (Michael et al. 2003), where breakup of cohesionless objects rather than of monolithic ones, is predicted by the modeling of current fragment orbital distributions.

The close up views of asteroids do not as yet show collections of particles or the significant lumpiness expected of loose aggregates of particles. Most can be described as moderately smooth surfaces modified by craters and grooves (See Figure 1). Some of the

radar data may be the best direct evidence of contact binaries. However, the radar images do not yet show multiple lumpiness; rather the second order features appear to be impact craters. Some asteroids that have a constriction in their shapes, such as Ida, that might be thought to be two pieces accumulated together with smaller sized particles filling in (Thomas et al 1996). However, in the instance of Ida, there is high resolution imaging in the constricted area, and it shows no evidence of any disturbance of loose material that relatively fine-grained fill between two large pieces might show as a result of impacts on one or the other of the large pieces.

Porosity

Porosities of asteroids and small satellites can be estimated using their mean density, estimated composition, and grain densities of analog meteoritic materials (see Britt et al. 2002). Mean density calculations require good measures of volumes and mass determinations. Masses for several asteroids have been determined by observations of the periods and sizes of orbits of natural satellites (Merline et al. 2002). Mean densities of asteroids range from slightly above 1.0 g cm^3 to 3.4 g cm^3 (Hilton 2002). Modeled total porosities range from 10-70%. The total porosity includes microporosity that has little structural effect; macroporosity (Britt et al 2002; Wilkison et al 2002) is mostly caused by, and affects, impact and other structural processes. Several asteroids, including 433 Eros, have estimated porosities of less than 30%. This is approximately the value at which materials are expected to lose coherency (Britt et al 2002). They are thought to be heavily fractured, but not to have been dispersed and reassembled in catastrophic collisions.

Center of mass-center of figure offsets: significance for structure

The relative positions of center of mass and center of figure, or more generally, the predicted and observed gravity fields, may help constrain interior models of small asteroids. Only for Eros do we have the gravity and shape data that allow any meaningful comparison. Although different techniques yield different locations of the center of figure, the offset of center of mass and center of figure for Eros is small: between 10 and 50 m (Konopliv et al 2003; Thomas et al 2002). The direction of offset does not fit any simple layer model based on the global planar structures (Thomas et al 2002), and can be matched by fairly small variations in mean density that might be due to modest changes in porosity. Certainly no great variation in composition through the asteroid is indicated, and would be inconsistent with the globally uniform spectral and color data (Bell et al 2002).

For Ida we do not have a gravity map, but the coincidence of the spin pole with the maximum moment of inertia of the shape, assuming homogeneous density distribution, suggests there are no major density variations within the object. As noted above, there is a strong suggestion of major structural feature in Ida; but it does not apparently separate areas of different density.

7. Morphology of surface expressions of structures

The surface expressions of structural features on small bodies can be largely classified as grooves, troughs, ridges, and crater shape modifications. They occur over a wide range of scales. The majority appears to represent surface disturbances in regolith overlying fractures in a competent substrate, but some ridges and troughs are large

enough to be visible at a global scale, and probably result from significant tectonic events.

Grooves

Grooves appear to be a common feature of small bodies, as they have been observed on Gaspra, Ida, Eros and Phobos. The grooves on these bodies share a range of surprisingly similar morphological types, from linear, straight-walled depressions, to rows of coalesced pits, but nearly all are less than 100 m in depth and are concave up (Fig. 5). Images of Phobos and Eros are of sufficient resolution to discriminate rows of discrete pits, and floors of grooves that may be smooth or hummocky. On all of these bodies, grooves are present in patterns that crosscut or otherwise intersect with each other.

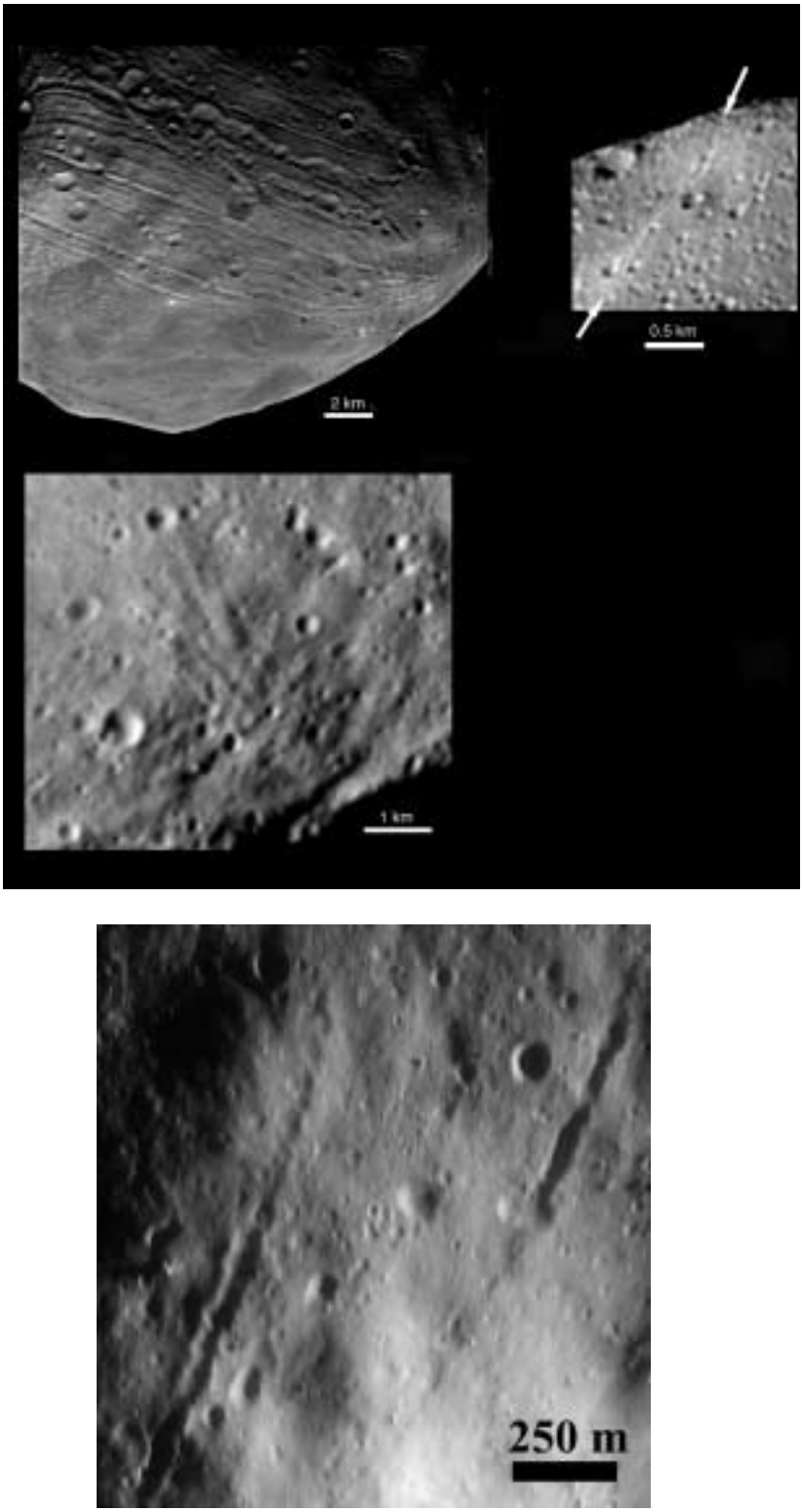

Figure 5 Grooves on small satellites and asteroids. a:: Phobos, b Ida, c: Gaspra, d: Eros.

The primary distinguishing feature of grooves among these small bodies is scale. Phobos' grooves are many kilometers long, and at least one can be traced for a distance of over 30 km. They are typically 100 – 200 m wide, and 10 – 20 m deep. They are grouped in four sets, each of which has parallel members (Thomas et al., 1979). Ida's grooves are < 4 km, with the majority less than 100 m wide. They are estimated to be under 50 meters in depth. Ida's grooves are concentrated in three regions; however, they are not obviously related to one crater or structural grain (Sullivan et al., 1996). Grooves on Gaspra are generally 100-200 m wide, 0.8 to 2.5 km long, and 10-20 m deep. Most occur in two groups of nearly parallel members, the most prominent of which roughly parallels the long axis of the body. There is no obvious connection to specific impact features (Veverka et al. 1994). The majority of grooves on Eros are up to 2 km long (although most are less than 800 m), with typical widths of 75 – 100 m. Depths are in the range of a few meters for smaller grooves, and tens of meters for the largest structures (Veverka et al., 2000; Prockter et al., 2002). Eros has grooves distributed unevenly across its surface. The highest concentration is of parallel grooves are within the concavity of the largest impact feature, Himeros. There are no obvious distributions of grooves around impact features.

Troughs

We distinguish troughs from grooves by their greater widths and depths, and high density of superposed craters and accompanying subdued morphology. The largest structural features on Eros are part of the Calisto Fossae, two parallel adjacent troughs separated by a narrow ridge. The troughs are several km long, range from 500-700m

wide, and are up to 120 m deep. They appear to be very old, with hummocky, degraded interiors and several large impact craters superimposed upon them. They have relatively flat floors, to within ±20 m, and many subparallel fractures are present both within the floors and adjacent to the troughs. The Calisto Fossae troughs have a morphology consistent with graben, and they may have formed by extension early in Eros' visible history.

Ridges

Elongate, positive relief forms that are not part of crater rims are found on Eros, and a few examples are found on Gaspra. Close-packed grooves have intervening crests that can appear to be ridges, but which we do not include in this discussion. The term Dorsum is also applied to a form on Ida, such as Townsend Dorsum, but as shown in Figure 4, this feature probably reflects differential response to fragmentation rather than being a strain-related form.

One of the most prominent features on Eros is Rahe Dorsum (IAU: Hinks Dorsum), an 18-km long arrangement of segments of somewhat varying morphology (Figs 3 and 6). This path curves around the central "waist " of the asteroid and comes close to the north pole.

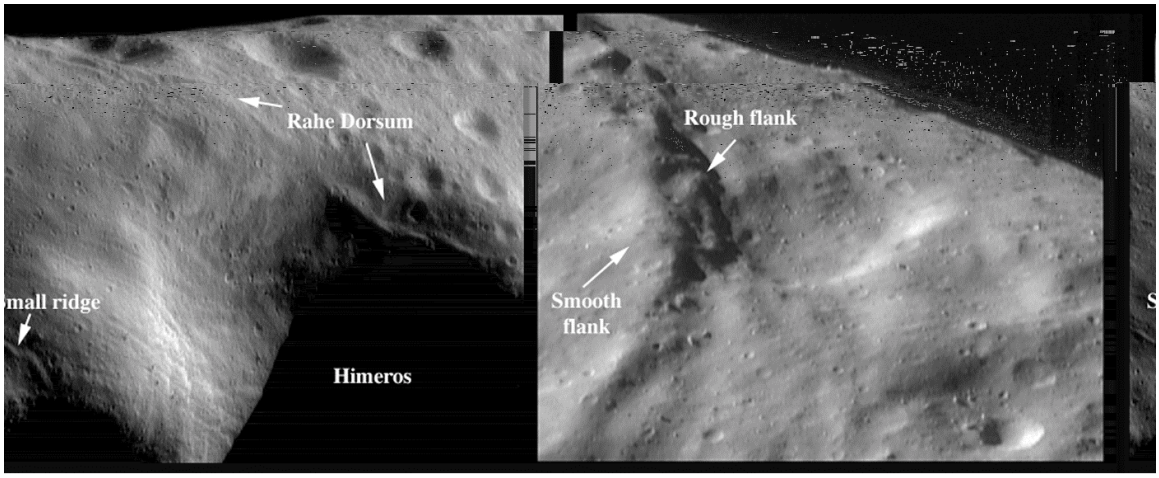

Figure 6 (a) Segment of Rahe Dorsum trending from the crater Himeros across the northern hemisphere. A small subparallel ridge is visible on the opposite side of Himeros. (b) In this segment, one flank of Rahe Dorsum is relatively smooth and at a low slope, while the opposite flank is much steeper and rougher textured, a morphology indicative of a thrust fault. MSI image 133972060; image width ~2.3 km. The contact between the dark and bright areas in the upper right is the limb of the asteroid.

Rahe Dorsum is comprised of a string of en echelon, asymmetric segments, with a variety of morphological characteristics. All segments are generally less than 300 m wide, and a few tens of meters in height. A notable exception is a scarp at the Himeros end of the ridge, which exhibits a near vertical drop of 120 m into an adjacent trough. Bright material at the foot of this scarp is interpreted to be material that has moved downslope by analogy to materials seen in other crater walls and talus observed around other scarps.(Fig. 7).

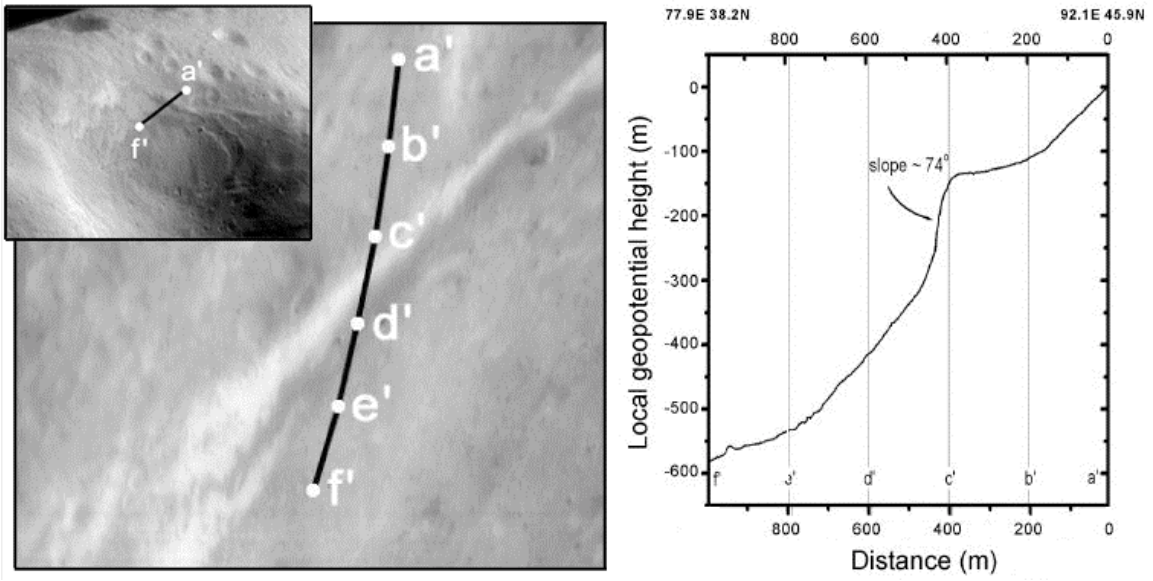

Fig. 7: NEAR Laser Ranger profile across Rahe Dorsum. Note that profile does not cross exactly perpendicular to the ridge, which is therefore steeper than the slope shown here (Adapted from the NEAR Image of the Day website).

Some segments are asymmetric in cross section: the more northerly flank has a relatively gentle slope and smooth surface, while the other flank is steeper and significantly rougher textured. The best example of this morphology occurs near Eros' north pole, where the ridge has the characteristics of a thrust fault, in which the steeper flank corresponds to the hanging wall face (Fig 6), (Prockter et al., 2002). Near Laser Ranger profiles across the ridge are consistent with this interpretation, and further suggest a succession of fault blocks (Cheng et al., 2002). At its Himeros terminus, Rahe Dorsum intersects a series of shallow troughs, while at the Psyche terminus, it appears to continue as a series of closely-spaced fractures, which themselves intersect with at least two other subparallel fractures sets. [louise: interpretation of the ends vs the rest of Rahe D?]

Although there are some impact craters on Rahe Dorsum, these are generally small, indicating that it may have formed in the latter stages of the asteroid's evolution, after any large crater formation. Superposition relationships between the ridge and the large craters Himeros and Psyche imply that it postdates these features. However, Rahe Dorsum is itself crosscut by a prominent groove, indicating that tectonic activity persisted subsequent to its formation (Prockter et al., 2002). The presence of fine-scale material on and at the foot of the ridge flanks suggests that it has undergone relatively recent mass wasting, possibly in response to seismic shaking from impacts elsewhere on the asteroid.

At least two smaller ridges are present in the same vicinity as Rahe Dorsum, but neither are longer than a few km. One of these is subparallel to Rahe Dorsum, but is on the opposite rim of Himeros (Fig. 6), and may have formed in response to the same stresses which caused Rahe Dorsum to be thrust above the surface.

Crater shape modification

Some craters on Eros have "squared off" outlines, a form which is controlled by joints, faults or other fabric within the target rock (Prockter et al., 2002). This type of structural control is seen in Arizona's Barringer Meteor crater, the outline of which is the result of two sets of orthogonal vertical joints in the underlying sedimentary rock (Shoemaker, 1963). The final crater shape was influenced by planes of weakness that were exploited by the cratering flow. The joints are oriented at approximately 45° to the sides of the crater as a result of the way excavation flow exploits fracture weaknesses. Although crater side orientations have not been mapped for Eros, locally several craters can have similar orientations of straight segments of crater walls, suggesting consistent fracture/joint orientations over a couple of kilometers extent.

8. Implications of grooves for structure and material properties

Several hypotheses have been proposed for the formation of grooves on small bodies. An early suggestion was that they are chains of secondary craters (Veverka and Duxbury, 1977), but this is not supported by observations of their morphology or their patterns. Most grooves lack raised rims, are linear in nature, and have uniform sizing and spacing of pits. These characteristics are difficult to match with expectations of secondary crater morphologies. Their patterns also do not match expectations from rolling ejecta (Thomas 1999).

The presence of blocks on the surface of Ida, Phobos, and Eros, are indicative of significant regolith retention on those bodies (Lee et al., 1996; Thomas et al., 2000; 2002). It is likely that the majority of grooves represent the disturbance of this regolith over deep, steeply dipping fractures or fracture zones (Thomas et al., 1979). Two models have been suggested for how this would occur. The first involves the ejection of material from fractures, probably through gas venting from the subsurface. This could occur if the body contains sufficient volatiles, which would be driven off when heated by a large impact event. The resulting grooves would have raised rims and shallow cross-profiles, from redeposition of material back into the groove, or slumping of the groove wall itself. However, it is not certain that sufficient amounts of bound water are present in the bodies in question, and few of the grooves actually have raised rims. If gas venting has occurred, it is likely to have been only a minor factor in groove development.

A more probable model for groove formation involves the drainage of regolith into fractures. Experimental modeling of this process suggests a series of steps occur in

the formation of grooves (Horstman and Melosh, 1989). These are: (a) the formation of a shallow trough over a fracture; (b) some local deepening, leading to early pits within the trough; (c) the existing pits become better developed, and new pits form; (4) neighboring pits meet, marking the beginning of groove formation, and (5) the pits coalesce, forming a prominent groove. Comparison of the model results to grooves on small bodies shows remarkable similarities. It has been noted that the fractures are probably deep, since individual grooves retain a planar pattern across vertical changes in topography of over 1 km (Thomas et al. 1979).

If grooves do form by this method, their tendency to have a preferred width could result from a uniform spacing or depth of fractures, or a uniform depth of regolith. The pits have a characteristic spacing, which corresponds to the thickness of the material layer in which they form, if it is dry, unconsolidated, and noncohesive. Perhaps surprisingly, this spacing appears to be uninfluenced by grain shape, size, rounding, angle of repose, or regolith bulk density (Horstman and Melosh, 1989), allowing a crude estimate of the regolith ldepth to be made for small bodies. For Phobos, pit spacing suggests the regolith is up to 100 m in depth (Thomas et al. 2000), while for Eros it is at least 30 m (Prockter et al., 2002). Both of these values are supported by other estimates of regolith thickness, based on morphology and topography.

9. Patterns of linear features and inferred structures

If grooves represent disturbances in regolith overlying fractures, the question remains of how the underlying fractures form. The geometric patterns of grooves or ridges in relation to likely stress orientations is the primary tool for inferring their origins as our data are all from remote sensing, although morphology of grooves and ridges

might help in determining displacements or associations. The most likely sources of stress, impacts and tidal effects, have been discussed above in Section 3.

Phobos grooves: Impact and/or Tidal stresses?

The grooves on Phobos were the first evidence found of small body structure in early Viking Orbiter images obtained in 1976. Subsequent data and study has shown them to likely be related to both impact and tidal influences.

The grooves on Phobos have a strong morphologic association with crater Stickney, which is ~10 km in diameter (over 40% of the mean diameter of Phobos), while their orientations are closely tied to the principal axes of the satellite. Phobos' grooves are widest and deepest near Stickney, and are virtually absent from the region of the satellite roughly opposite this crater. The grooves are also consistent with forming at about the same time as Stickney, based on crater counts and relative crispness of the topography of the crater and the grooves.

However, the geographic pattern of the grooves suggests an important role for stresses unrelated to Stickney (Fig. 6). A large fraction of the Phobos grooves are grouped into sets of parallel members, with paths that follow the intersection of planes with the surface. Normals to these planes lie very close to the plane defined by the longest and shortest axes of the satellite. Because the satellite is in synchronous rotation about Mars, tidal stresses are essentially fixed with respect to the body of the satellite. These forces are extensional along the long axis of the satellite, and the resulting stress fields are consistent with fracturing in planes similar to the groove-defined ones (Aggarwal and Oberbeck 1974; Dobrovolskis 1982).

This combination of associations has complicated interpretations of the grooves.

Burns (1978) proposed that the grooves on Phobos could have formed by fracturing which occurred when Phobos was captured by Mars. The morphologic association with the large crater led to suggestions that the grooves are related to Stickney's formation (Veverka et al., 1977; Thomas et al., 1978, 1979). Soter and Harris (1977) proposed the grooves formed through tidal stressing of the satellite by Mars as the satellite evolved inward toward Mars. Weidenschilling (1979) made calculations that demonstrated the sequence of development of tidal-induced fractures could vary considerably with different shapes. He suggested that a large impact such as Stickney could have broken the satellite's synchronous rotation, and stresses associated with recovery to synchronous spin might have caused the groove fracture pattern. One aspect of tidal stresses does not fit well with the apparent ages of the grooves. The grooves have a modest population of superposed craters. Tidal stresses increase as a^{-3}, where a is the satellite's semimajor axis. Thus the stresses would increase progressively more rapidly as the satellite orbit shrinks. Thus tidal fracturing by itself would be expected to be recent, or increasingly prominent, whereas the grooves are not the most recent features on the satellite.

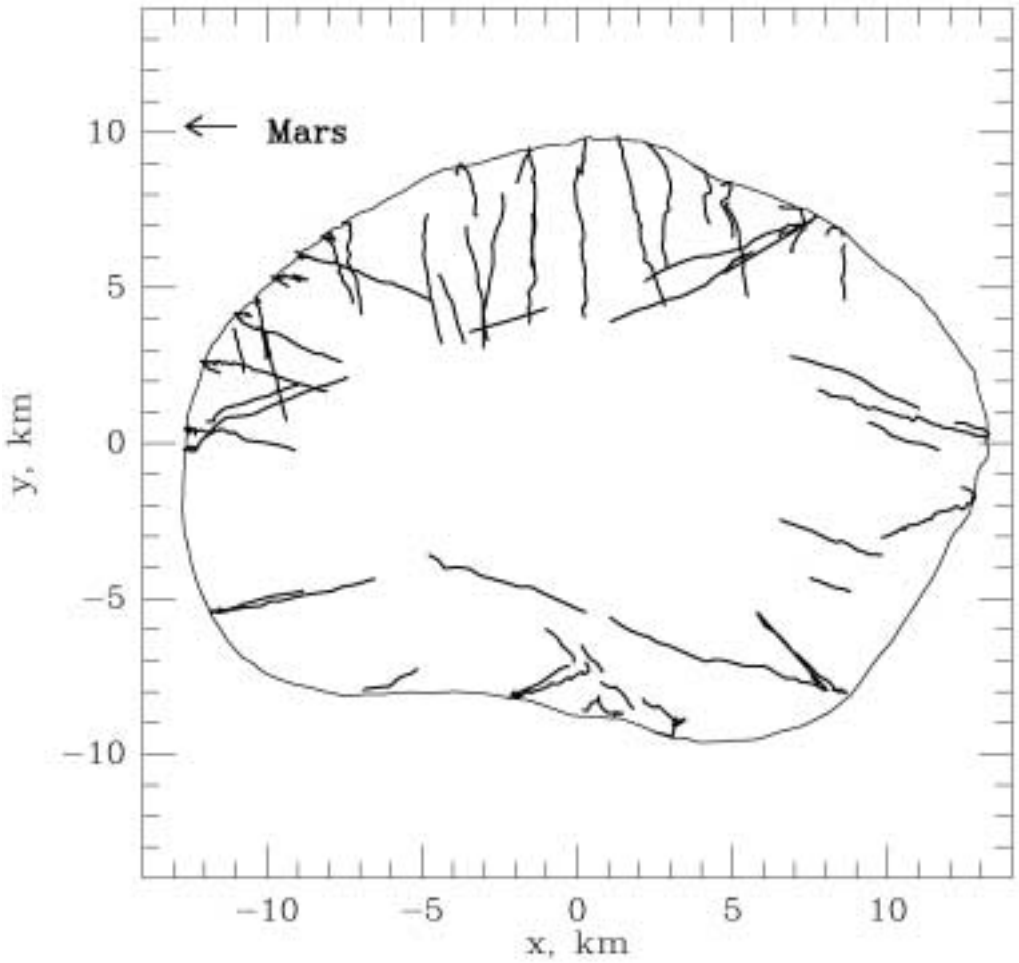

Figure 8. Projection of prominent grooves on Phobos, looking from 0N, 270W, along the direction of orbital motion.

Modeling of the Stickney impact by Asphaug and Melosh (1993) predicted that an event of this magnitude could fracture the interior of Phobos on a scale of several kilometers, a value consistent with the extent of the grooves. The predicted fragment sizes were consistent with groove spacing, which, with the attendant assumptions, would suggest that Phobos was coherent prior to the impact. However, the strong association of

groove pattern with expected tidal effects suggests that whatever the role of impact stresses, the tidal field helped define the principal stresses responsible for groove fractures. Given the magnitude of the impact stresses compared to the weak tidal ones, tidally-driven fracturing in a weak Phobos may have been exploited by the impact, rather than formed entirely new. While it may appear counter-intuitive that a weak object would not show dominant effects of a very large impact, findings from the porous asteroid Mathilde may be relevant. A weak, fractured target can absorb much of the impact energy by inefficient transmission of the seismic energy, and by a large fraction of the crater being produced by compression rather than excavation (Housen et al. 1999). Damage outside the visible crater is minimized. Thus, a Phobos weak enough to be fractured by tides could still suffer a large impact that could widen the fractures, but may not drastically rearrange the object.

Eros structures: no single pattern

The Eros grooves provide a strong contrast to the global organization of the ones on Phobos. (Figs. 7, 8) They are not obviously related to specific craters, nor do they cluster in orientations related to the overall shape of the object. There is a global pattern only in the sense noted earlier that Rahe Dorsum and Calisto fossae may reflect a global planar fabric. The grooves do maintain consistent morphologic and orientation patterns over areas of several km, such as between 300-330°W and 0-30°N, and 20-90°W, 60-30°S (Fig. 7). These patterns suggest mechanical continuity over a few km. Additionally, the lack of obvious relation to any individual craters suggests many fractures might result from seismic focusing or reactivation from later impact events.

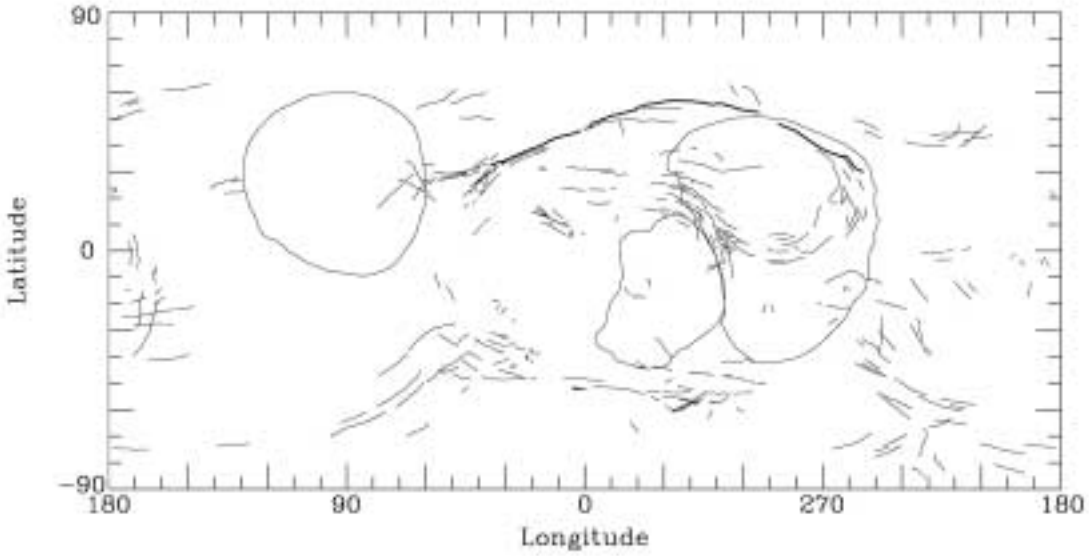

Figure 9. Map of grooves and ridges on Eros; simple cylindrical projection, which greatly expands the relative area of regions near longitude 90 and 270. Outlines of the three largest craters, from left to right, Psyche, Shoemaker, and Himeros are shown for reference. Most features plotted are grooves, but ridges, such as the heavy line marking Rahe Dorsum, are included.

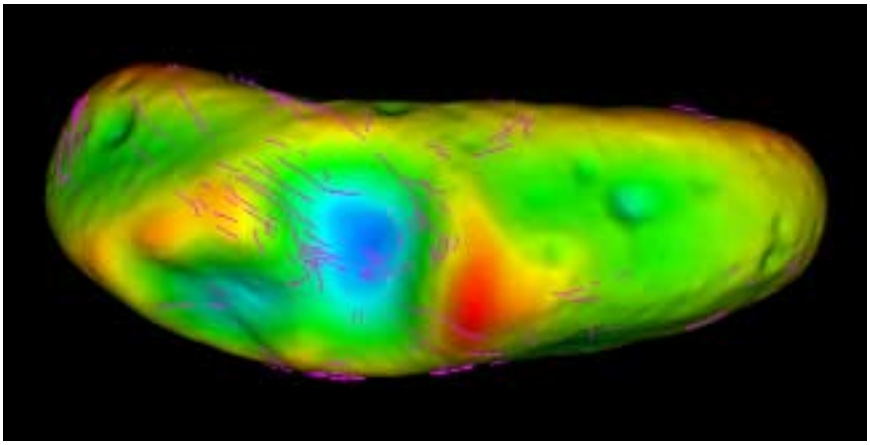

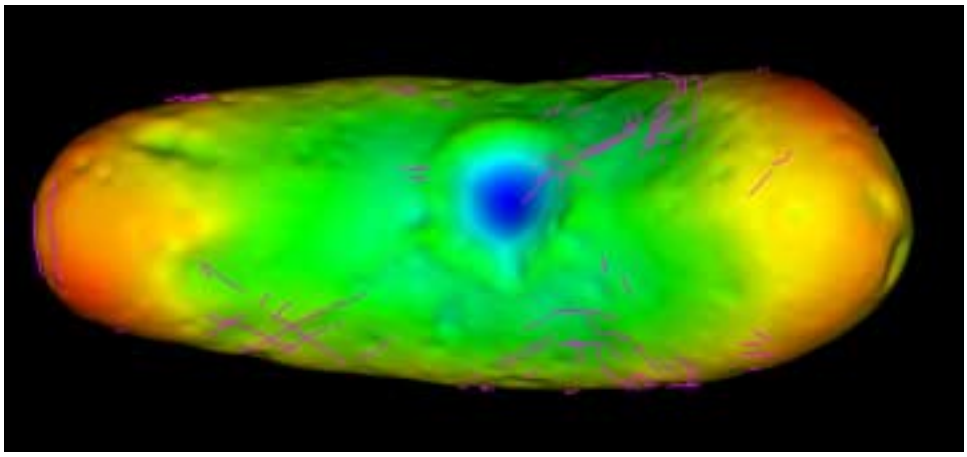

Figure 10 Views of linear features on Eros. Heights relative to equipotential surface represented by color; red high, blue low.

The morphologic association of the grooves on Phobos with a large crater, and with obvious fracture patterns, and modeling of impact fracturing (Asphaug and Melosh, 1993, and others) raised the possibility that grooves would reflect a variety of asteroid

structures. Grooves have been used as a crude seismological record of impact activity (Asphaug et al., 1996), a method first applied to Phobos (Fujiwara, 1991; Asphaug and Melosh, 1993; Asphaug and Benz, 1994), and since been applied to Ida (Asphaug et al., 1996).

Comparison of likely crater-induced fracturing on these small objects to terrestrial examples is complicated by the greatly different gravity regimes and uncertainty about the physical properties of the target objects. Numerical models have been used to simulate impacts into small bodies, and the results suggest that stresses may be focussed in regions far from the initial crater depending on internal structure and surface shape.

Ida grooves: antipodal effects?

Ida displays a modest collection of grooves, none of which are obviously concentrated about a particular crater. One set is essentially opposite the largest distinct concavity on Ida, a 15 km wide feature, Vienna Regio (Fig. 4). Using hydrocode techniques, Asphaug et al. (1996) showed that powerful stress waves from the Vienna Regio impact on Ida could have disrupted the surface at the opposite end of the asteroid, to form the Pola Regio grooves. The apparent freshness of the grooves implies that although they may have been originally formed by the Vienna impact, a somewhat degraded crater, they could have been subsequently reactivated by a later impact, probably crater Azzurra, which is about 10 km across and located about 15 km from the grooves. If fractures underlying grooves are formed through the focusing of seismic waves, then the body on which they appear must be sufficiently mechanically coupled to transmit seismic waves. This interpretation implies that such objects are not rubble piles, although they may have a measure of fracturing in their interiors.

Gaspra structures

Grooves on Gaspra are more globally organized (within the approximately 25% of the surface that is well-imaged) than those on Eros (Fig. 10). Most occur in what may be either two groups of slightly different orientations, or as part of a globally curving pattern. Thomas et al. (1994) showed that the grooves and some of the flat facets of the asteroid might follow structures parallel to a direction about 15˚ from the long axis of the asteroid. This could imply a structural fabric extending through much of Gaspra, which has affected its present shape. Gaspra also shows a few ridges that may be part of a curving pattern. Most notable among these is a ridge that deformed a small crater near the larger end of the object and was the first indication of compressive failure on a small object (Thomas et al. 1996).

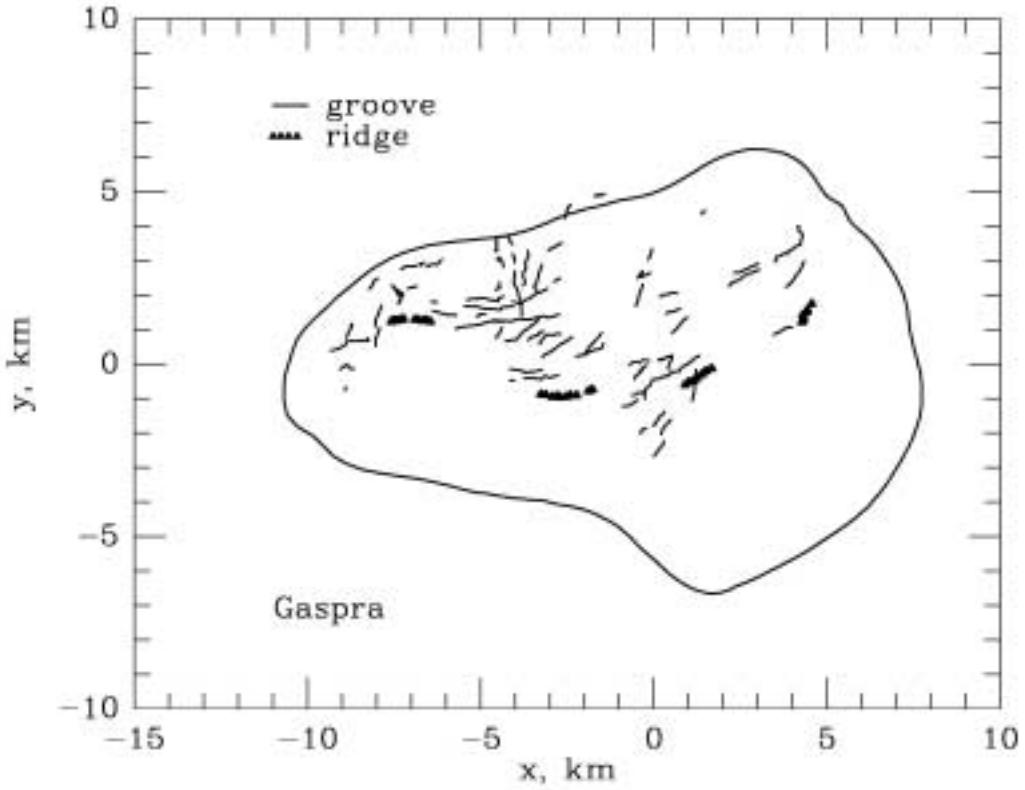

Figure 12. Gaspra groove and ridge patterns. Projection of positions from 90N, equatorial profile for reference. Pattern covers the well imaged area. Ridge at the right (4.5, 1.2) deforms a crater.

10. Overview and Outstanding questions

Objects that have no internally driven tectonics display a remarkable variety of forms generated by impacts and tidal stresses. Different compositions, different sizes, and different orbital histories may explain much of this variety.

Our knowledge of the tectonics and structures of small bodies is demonstrably crude at the moment. The limitations of a few examples of remote sensing of objects covered by loose debris in interpreting interior features is all too clear. Yet our

experience is sufficient to pose questions in ways that future missions may provide more definitive answers. These interior views are still important in evaluating the assembly and evolution of solar system objects.

The clear evidence of many styles of fracturing and a wide variety of porosities in these objects should allow design of seismic and radar sounding probes of the interiors. Better estimates of regolith cover can help position active and passive interior investigations. The Deep Impact mission will actively expose the interior of a comet and investigate interior structures and compositions with a variety of techniques to examine the crater and the evolution of materials ejected from it. More successful associations of meteorites with specific asteroids will help place the structures in more specific contexts.

Glossary:
Regolith
Asteroid
gravitational slopes
Astronomical unit (AU)

Table 1: Spacecraft remote sensing data of small bodies.

OBJECT	PRIMARY	MEAN RADIUS, KM	MISSION	PIXEL SCALE RANGE
Satellites:				
Phobos	Mars	11	Viking 1976-1980	6-100+m
Deimos	Mars	6	Viking 1976-1980	3-100+m
Janus	Saturn	86	Voyager 1980-1981	3 –6 km
Epimetheus	Saturn	55	Voyager 1980-1981	1.6 – 6 km
Proteus	Neptune	140	Voyager 1989	1.6 km
Asteroids:				
Gaspra		6.1	Galileo 1991	64-500 m
Ida		15.7	Galileo 1993	31-500 m
Mathilde		26.5	NEAR 1997	240-1200 m
Eros		8.3	NEAR 2000-2001	0.1-100 m
Comets:				
Halley		6	Giotto, Vega 1986	150 m
Wild-2		2	Stardust 2004	15 m
Borrelly		3	DS-1 2001	60 m

References

Aggarwal, H. R. and V. R. Oberbeck, 1974: Roche limit of a solid body. *Astrophys. Jour.*, **191**, pp. 577–588.

A'Hearn, M. F., Millis, R. L., Schleicher, D. G., Osip, D. J., and Birch, P. V. 1992. The ensemble properties of comets: Results from narrow band photometry of 85 comets, 1976-1992. *Icarus* **118,** 223-270.

Asphaug, E. and W. Benz, 1996: Size, density and structure of comet Shoemaker-Levy 9 inferred from the physics of tidal breakup. *Icarus*, **121**, pp. 225-248.

Asphaug E. and Melosh H. J., 1993: The Stickney impact of Phobos: A dynamical model. *Icarus*, **101**, pp. 144–164.

Asphaug, E., J. M. Moore, D. Morrison, W. Benz, M. C. Nolan, and R. J. Sullivan, 1996: Mechanical and geological effects of impact cratering on Ida. *Icarus*, **120**, pp. 158–184.

Asphaug E., Ostro S. J., Hudson R. S., Scheeres D. J, and Benz W., 1998: Disruption of kilometre-sized asteroids by energetic collision. *Nature*, **393**, pp. 437–440.

Bell, J. F., D. R. Davis, W. K. Hartmann, and M. J. Gaffey, 1989: Asteroids: The big picture. In *Asteroids II* [R. P. Binzel, T. Gehrels, and M. S. Mathews, (eds)], Univ. of Arizona Press, Tucson, pp. 921–945.

Bell, J. F. III, N. Izenberg, P. G. Lucey, B. E. Clark, C. Peterson, M. J. Gaffey, J. Joseph, B. Carcich, A. Harch, M. E. Bell, J. Warren, . D. Martin, L. A. McFadden, D.

Wellnitz, S. Murchie, M. Winter, J. Veverka, P. Thomas, M. S. Robinson, M. Malin, and A. Cheng, 2002: Near-IR reflectance spectroscopy of 433 Eros from the NIS instrument on the NEAR mission. 1. Low phase angle observations. *Icarus*, **155**, pp. 119–144.

Binzel, R. P., and S. Xu, 1993: Chips off of asteroid 4 Vesta: Evidence for the parent body of achondritic meteorites. *Science*, **260**, pp. 186–191.

Binzel, R. P., M. A'Hearn, E. Asphaug, M. A. Barucci, M. Belton, W. Benz, A. Cellino, M. Festou, M. Fullchignoni, A. W. Harris, A. Rossi, and M. T. Zuber, 2003. Interiors of small bodies: foundations and perspectives. *Planetary and Space Sci.* **51**, 443-454.

Bottke W. F. Jr., Richardson D. C., and Love S. G., 1997: Can tidal disruption of asteroids make crater chains on the Earth and Moon? *Icarus*, **126**, pp. 470–474.

Bottke W. F. Jr., Richardson D. C., Michel P., and Love S. G., 1999: 1620 Geographos and 433 Eros: Shaped by planetary tides? *Astron. J.*, **117**, pp. 921–1928.

Britt D. T. and Consolmagno G. J., 2001: Modeling the structure of high-porosity asteroids. *Icarus*, **152**, pp. 134–139.

Britt, D. T., D. Yeomans, K. Housen, and C. Consolmagno, 2002: Asteroid density, porosity, and structure. In *Asteroids III* [Bottke, W., A. Cellino, P. Paolicci, and R. Binzel, (eds)], Tucson, Univ. of Arizona Press, pp. 485–499.

Burns, J.A., 1978: The dynamical evolution and origin of the martian moons. *Vistas Astron.*, **22**, pp. 193–210.

Chapman, C. R. and W. McKinnon, 1986: Cratering of planetary satellites. In *Satellites* [J. Burns and M. Mathews (eds)], Univ. Arizona Press, Tucson, pp. 492–580.

Chapman C. R., Merline W. J., and Thomas P., 1999: Cratering on Mathilde. *Icarus*, **140**, pp. 28–33.

Cheng, A. F., O. Barnouin-Jha, L. Prockter, M. T. Zuber, G. Neumann, D. E. Smith, J. Garvin, M. Robinson, J. Veverka, and P. Thomas, 2002: Small-scale topography of 433 Eros from laser altimetry and imaging. *Icarus*, **155**, pp. 51–74.

Croft, S. K., 1992: Proteus: Geology, shape, and catastrophic destruction. *Icarus*, **99**, pp. 402–419.

Dobrovolskis, A., 1982: Internal stresses in Phobos and other triaxial bodies. *Icarus*, **52**, pp. 136–148.

Dombard, A.J. and A.M. Freed, 2002: Thermally induced lineations on the asteroid Eros: Evidence of orbit transfer. *Geoph. Res. Lett.*, **29**, 10.1029/202GL015181.

Duennebier, F., 1976: Thermal movement of the regolith. In *Proceedings of the 7th Lunar Science Conf.*, Peramon, Oxford, pp. 1073–1086.

Durda D. D., 1996: The formation of asteroidal satellites in catastrophic collisions. *Icarus*, **120**, pp. 212–219.

Fujiwara, A., 1991: Stickney-forming impact on Phobos: Crater shape and induced stress distribution. *Icarus*, **89**, pp. 384–391.

Gault, D. E., W. L. Quaide, and V. R. Oberbeck, 1968: Impact cratering mechanics and structures in shock metamorphism of natural materials [B. M. French and N. M. Short (eds)]. Mono Book Co., Baltimore Md., pp. 87–99.

Gradie, J. C. and E. F. Tedesco, 1982: Compositional structure of the asteroid belt. *Science*, **216**, pp. 1405–1407.

Grimm, R. E. and H. Y. McSween, 1993: Heliocentric zoning of the asteroid belt by aluminum-26 heating. *Science*, **259**, pp. 653–655.

Hilton, J. L., 2002: Asteroid masses and densities. In *Asteroids III* [Bottke, W., A. Cellino, P. Paolicci, and R. Binzel, (eds)]. Tucson, Univ. of Arizona Press, pp. 103–112.

Housen K. R., Holsapple K. A., and Voss M. E., 1999: Compaction as the origin of the unusual craters on asteroid Mathilde. *Nature*, **402**, pp. 155–157.

Horstman, K. C., and H. J. Melosh, 1989: Pits in cohesionless materials: Implications for the surface of phobos. *Icarus*, **94**, pp. 12,433–12,441.

Hudson, R. S., S. J. Ostro, and D. J. Scheeres, 2003. High resolution model of asteroid 4179 Toutatis. *Icarus* **161**, 346-355.

Johnson, T. V. and T. R. McGetchin, 1973: Topography on satellite surfaces and the shape of asteroids. *Icarus*, **39**, pp. 317–351.

Keil, K., 2002: Geological history of asteroid 4 Vesta: the "smallest terrestrial planet". In *Asteroids III* [Bottke, W. et al. (eds)], pp. 573–584.

Konopliv, A. S., J. K. Miller, W. M. Owen, D. K. Yeomans, J. D. Giorgini, R. Garmier, and J.-P. Barriot, 2002: A global solution for the gravity field, rotation, landmarks, and ephemeris of Eros. *Icarus*, **160**, pp. 289–299.

Lee, P., J. Veverka, P.C. Thomas, P. Helfenstein, M.J.S. Belton, C.R. Chapman, R. Greeley, R.T. Pappalardo, R. Sullivan, and J.W. Head III, 1996: Ejecta blocks on 243 Ida and on other asteroids. *Icarus*, **120**, pp. 87–105.

Love S. G. and Ahrens T. J., 1996: Catastrophic impacts on gravity dominated asteroids. *Icarus*, **124**, pp. 141–151.

Margot, J.-L., M. C. Nolan, L. A. M. Benner, S. J. Ostro, R. . Jurgens, J. D. Giorgini, M. A. Slade, and D. B. Campbell, 2002: Binary asteroids in the near-Earth object population. *Science*, **296**, pp. 1445–1448.

McKinnon W. B. and Schenk P. M., 1995: Estimates of comet fragment masses from impact crater chains. *Geophys. Res. Lett.*, **22**, pp. 1829–1832.

McSween, H. Y. Jr., A. Ghosh, R. E. Grimm, L. Wilson, and A. D. Young, 2002: Thermal evolution models of asteroids. In *Asteroids III* [W. Bottke et al., (eds)]. Univ. of Arizona Press, Tucson, pp. 559–571.

McCoy, T. J., T. H. Burbine, L. A. McFadden, R. D. Starr, M. J. Gaffey, L. R. Nittler, N. Izenberg, P. Lucey, J. I. Trombka, J. F. Bell III, B. E. Clark, P. E. Clark, S. W. Squyres, C. R. Chapman, W. V. Boynton, and J. Veverka, 2001: The composition of 433 Eros: A mineralogical-chemical synthesis. *Meteoritics and Planetary Science*, **36**, pp. 1661–1672.

Melosh, H. J., 1989: *Impact cratering*. Oxford Univ. Pres, New York. 245 pp.

Melosh H. J. and Ryan E. V., 1997: Asteroids: Shattered but not dispersed. *Icarus*, **129**, pp. 562–564.

Melosh H. J. and Schenk P., 1993: Split comets and the origin of crater chains on Ganymede and Callisto. *Nature*, **365**, pp. 731–733.

Merline W. J., Weidenschilling S. J., Durda D. D., Margot J.-L., Pravec P., and Storrs A. D., 2002: Asteroids do have satellites. In *Asteroids III* [W. F. Bottke Jr. et al, (eds)]. Univ. of Arizona Press, Tucson, pp. 289–312.

Michel, P., W. Benz, and D. C. Richardson, 2003: Disruption of fragmented parent bodies as the origin of asteroid families. *Science*, **421**, pp. 608–611.

Nicholson, P. D., D. P. Hamilton, K. Matthews, and C. F. Yoder, 1992: New observations of Saturn's coorbital satellites. *Icarus*, **100**, pp. 464–484.

Ostro S. J., Hudson R. S., Nolan M. C., Margot J., Scheeres D. J., Campbell D. B., Magri C., Giorgini J. D., and Yeomans D. K., 2000: Radar observations of asteroid 216 Kleopatra. *Science*, **288,** pp. 836–839.

Pravec P. and Harris A. W., 2000: Fast and slow rotation of asteroids. *Icarus*, **148**, pp.12–20.

Prockter, L., P. Thomas, M. S. Robinson, J. Joseph, A. Milne, B. Bussey, J. Veverka, and A. Cheng, 2002: Surface expressions of structural features on Eros. *Icarus*, **155**, pp. 75–93.

Richardson, D. C., Z. M. Leinhardt, H. J. Melosh, W. F. Bottke Jr., and E. Asphaug, 2002: Gravitational aggregates: Evidence and evolution. In *Asteroids III* [Bottke et al., (eds)]. Univ. of Arizona Press, Tucson, pp. 501–51.

Robinson, M. S., P. C. Thomas, J. Veverka, S. L. Murchie, and B. B. Wilcox, 2002: The geology of 433 Eros. *Meteoritics and Planetary Science*, **37**, pp.1651–1684.

Shoemaker, E.M., 1963: Impact Mechanics at Meteor Crater, Arizona. In *The Moon, Meteorites, and Comets*, [B.M. Middlehurst and G.P. Kuiper, (eds)]. The Solar System, **4**, Univ. Chicago Press, Chicago/London, pp.301–336.

Soderblom, L. et al., 2002: Observations of comet 19P/Borrely by the Miniature Integrated Camera and Spectrometer aboard Deep Space 1. *Science*, **296**, pp. 1087–1091.

Sonnett, C. P., D. S. Colburn, and K. Schwartz, 1968: Electrical heating of meteorite parent bodies and planets by dynamo induction from a premain sequence T Tauri "solar wind." *Nature*, **219**, pp. 924–926.

Soter, S., and A. Harris, 1977: Are striations on Phobos evidence for tidal stress? *Nature*, **268**, pp. 421–422.

Sullivan, R., R. Greeley, R. Pappalardo, E. Asphaug, J.M. Moore, D. Morrison, M.J.S. Belton, M. Carr, C.R. Chapman, P. Geissler, R. Greenberg, J. Granahan, J.W. Head III, R. Kirk, A. McEwen, P. Lee, P.C. Thomas and J. Veverka, 1996: Geology of 243 Ida. *Icarus*, **120**, pp. 119–139.

Thomas, P. 1989: The shapes of small satellites. *Icarus*, **77**, pp. 248–277.

Thomas P. C., 1999: Large craters on small objects: Occurrence, morphology, and effects. *Icarus*, **142**, pp. 89–96.

Thomas, P., J. Veverka, and T. C. Duxbury, Origin of grooves on Phobos, 1978: *Nature*, **273**, pp. 282–284.

Thomas, P., J. Veverka, A. Bloom, and T. Duxbury, 1979: Grooves on Phobos: Their distribution, morphology, and possible origin, *J. Geophys. Res.*, **84**, pp. 8457–8477.

Thomas, P.C., J. Veverka, D. Simonelli, P. Helfenstein, B. Carcich, M.J.S. Belton, M.E. Davies and C. Chapman, 1994: The shape of Gaspra. *Icarus*, **107**, pp. 23–36.

Thomas, P.C., J. Veverka, R. Sullivan, D.P. Simonelli, M.C. Malin, M. Caplinger, W.K. Hartmann, and P.B. James, 2000: Phobos: Regolith and ejecta blocks investigated with Mars Orbiter camera images. *J. Geophys. Res.*, **105**, pp. 15,091– 5,106.

Thomas, P.C., J. Joseph, B. Carcich, J. Veverka, B.E. Clark, J.F. Bell III, A. W. Byrd, R. Chomko, M. Robinson, S. Murchie, L. Prockter, A. Cheng, N. Izenberg, M.

Malin, C. Chapman, L.A. McFadden, R. Kirk, M. Gaffey and P.G. Lucey, 2002: Eros: Shape, topography, and slope processes. *Icarus*, **155**, pp. 18–37.

Veverka, J., and T. Duxbury, 1977: Viking observations of Phobos and Deimos: Preliminary results. *J. Geophys. Res*., **82**, pp. 4213–4223.

Veverka, J., P. Thomas, D. Simonelli, M.J.S. Belton, M. Carr, C. Chapman, M.E. Davies, R. Greeley, R. Greenberg, J. Head, K. Klaasen, T.V. Johnson, D. Morrison and G. Neukum, 1994: Discovery of grooves on Gaspra. *Icarus*, **107**, pp. 72–83.

Veverka J. and 16 colleagues, 1997: NEAR's flyby of 253 Mathilde: Images of a C asteroid. *Science*, **278**, pp. 2109–2114.

Veverka, J., P. Thomas, A. Harch, B. Clark, J. F. Bell III, B. Carcic, J. Joseph, S. Muchie, N. Izenberg, C. Chapman, W. Merline, M. Malin, L. McFadden, and M. Robinson, 1999: NEAR encounter with asteroid 253 Mathilde: Overview. *Icarus*, **140**, pp. 3–16.

Weidenschilling, S. J., 1979: A possible origin for the grooves on Phobos. *Nature* **282**, pp. 697–698.

Weidenschilling S. J., 1981: How fast can an asteroid spin? *Icarus*, **46**, pp. 124–136.

Wilkison, S. L., M. S. Robinson, P. C. Thomas, J. Veverka, T. J. McCoy, S. L. Murchie, L. M. Prockter, and D. K. Yeomans, 2002: An estimate of Eros's porosity and implications for internal structure. *Icarus*, **155**, pp. 94–103.